FEDERAL UNIVERSITY OF TECHNOLOGY, AKURE
JOURNAL OF ENGINEERING AND ENGINEERING TECHNOLOGY

INVESTIGATING THE THERMODYNAMIC CHARACTERISTICS OF ENERGY SAVING REFRIGERATING SYSTEM WITH COLD ACCUMULATOR

[1]Ikem, I. A.[*], [2]Akintunde, M. A., [3]Titiladunayo, I. F. and [3]Awatt, E.

[1]Department of Mechanical Engineering, University of Cross River State, Calabar, Nigeria
[2]Department of Mechanical Engineering, Federal University of Technology, Akure, Ondo State, Nigeria
[3]National Center for Energy and Environment, Energy Commission of Nigeria, University of Benin

**Correspondence author: azors9kee@yahoo.com*

Ikem, I. A., Akintunde, M. A., Titiladunayo, I. F. and Awatt, E. (2025): Investigating the Thermodynamic Characteristics of Energy Saving Refrigerating System with Cold Accumulator**.** *FUTA Journal of Engineering and Engineering Technology /19(2), 41-48*

Received Date: 08.07.25 **Accepted Date: 15.10.25**

Abstract
This study investigates the thermodynamic characteristics of an energy-saving refrigerating system integrated with a cold accumulator. The purpose is to enhance system performance, reduce energy consumption, and improve temperature stability during fluctuating load conditions. The purpose is to enhance system performance, reduce energy consumption, and improve temperature stability during fluctuating load conditions. The experimental setup and theoretical analysis focus on evaluating the performance of the system under various operating parameters, including evaporating and condensing temperatures, accumulator charge–discharge cycles, and refrigerant mass flow rate. Key thermodynamic indicators such as Coefficient of Performance (COP) and energy savings potential were analyzed. From simulation, freezing ice above the thickness of 4 mm during the process of charging the accumulator led to an increase in charging time and a decrease in the mass of ice accumulated over 8 hours. The maximum thickness of ice obtained during the accumulation time, required lowest boiling point of the refrigerant, which is at $t_0 = -15℃$ and defrosting was carried out with ice thickness not more than 10 mm to avoid increasing the condensation temperature. Results show that incorporating a cold accumulator significantly improves system efficiency by optimizing compressor operation and reducing peak power demand. Reducing the condensation cycle temperature during the accumulation, reduces overall power consumption by 8 -10 % compared to the conventional system.

Keywords: *Coefficient of performance (COP), cold accumulator, system performance, heat exchanger, energy consumption.*

Introduction

Refrigeration systems are essential to numerous sectors; including food preservation, pharmaceuticals, and industrial processing, but they are also among the largest consumers of electric energy in many contexts (International Energy Agency (IEA), 2022). Under variable thermal loads, conventional vapour compression refrigeration cycles often operate under part-load conditions, which reduces efficiency and increases energy consumption (Dopazo *et al*., 2012). There is, therefore, growing interest in approaches that improve load matching, reduce energy waste, and smooth the operation of compressors to increase overall system performance (Chen *et al.,* 2018).

One promising technique is the use of cold accumulators or cold thermal energy storage (CTES), (Liu *et al.*, 2018). These devices store cooling capacity during periods of lower demand (or lower electricity cost) and release it during peak load periods, thereby enabling better utilization of the refrigeration system and reducing peak electricity draw (Chia-Sheng *et al*. 2025). Cold accumulators, using water or eutectic liquids, can improve compressor efficiency by avoiding frequent cycling and let refrigeration machinery run closer to full load (Yan *et al*., 2019).

Several recent studies have expanded on this concept, especially integrating phase-change materials for cold storage to enhance subcooling and improve cycle performance. For example, "Theoretical study on a vapor-compression refrigeration system with cold storage for freezer applications" shows improvements in COP and volumetric refrigeration capacity when PCM-based cold storage is used (International Energy Agency (IEA), 2022).

Despite this, there remain open questions around how various operating parameters affect the thermodynamic performance of systems with cold accumulators. Parameters such as the charge-discharge cycles of the accumulator, the temperature differentials between evaporator/condenser, refrigerant flow rates, and the dynamic load profiles (weekday vs. weekend, day vs. night) all interact in complex ways. Moreover, many existing studies are purely theoretical or simulation-based; fewer provide detailed experimental validation or explore real-world operating conditions. There is also limited literature on how cold-accumulator-augmented refrigeration performs in environments with unreliable power supply or fluctuating tariffs; situations common in many developing regions. One experimental study, "Experimental Investigation of a Chiller with Cold Accumulator Using the Vertical-Tube Evaporator Water Chiller" by Ikem *et al.* (2017), provides useful results but leaves room for further thermodynamic characterization across varied load conditions.

Therefore, this work aims to fill those gaps by investigating the thermodynamic characteristics of a refrigerating system with cold accumulator, through both theoretical analysis and experimental work. The objectives include quantifying improvements in coefficient of performance (COP), exergy efficiency, energy savings, and temperature stability under different operating conditions. Through this, the study seeks to provide guidance for design and optimization of energy saving refrigeration systems incorporating cold accumulators, especially in contexts where electrical supply, load demand, or energy cost vary significantly.

Materials and Experimental Procedures

Description of the Experimental Set-up

To study the processes occurring in the mock-up of a vertical-tube evaporator - water cooler, in the Kuban State Technological University (Krasnodar, Russia), we developed and manufactured an experimental stand, where 1 is an evaporator; 2 is condenser; 3 is condenser cooler; 4,5 are measuring containers; 6 is level indicator; 7 is tank with coolant; 8 is coolant pump; 9 is coolant flow meter; 10 is electric heater; 11 is refrigerant cylinder; 12 is vacuum pump; 13 is branch pipe; 14 is manometer; 15 is thermometer; 16 is safety valve; 17 is collector; 18 is refrigerant vapour pipeline; 19 is liquid refrigerant pipeline; 20 is liquid coolant pipeline; 21 is glass thermometer; 22 is regulating damper. The experimental stand is shown in Figure 1.

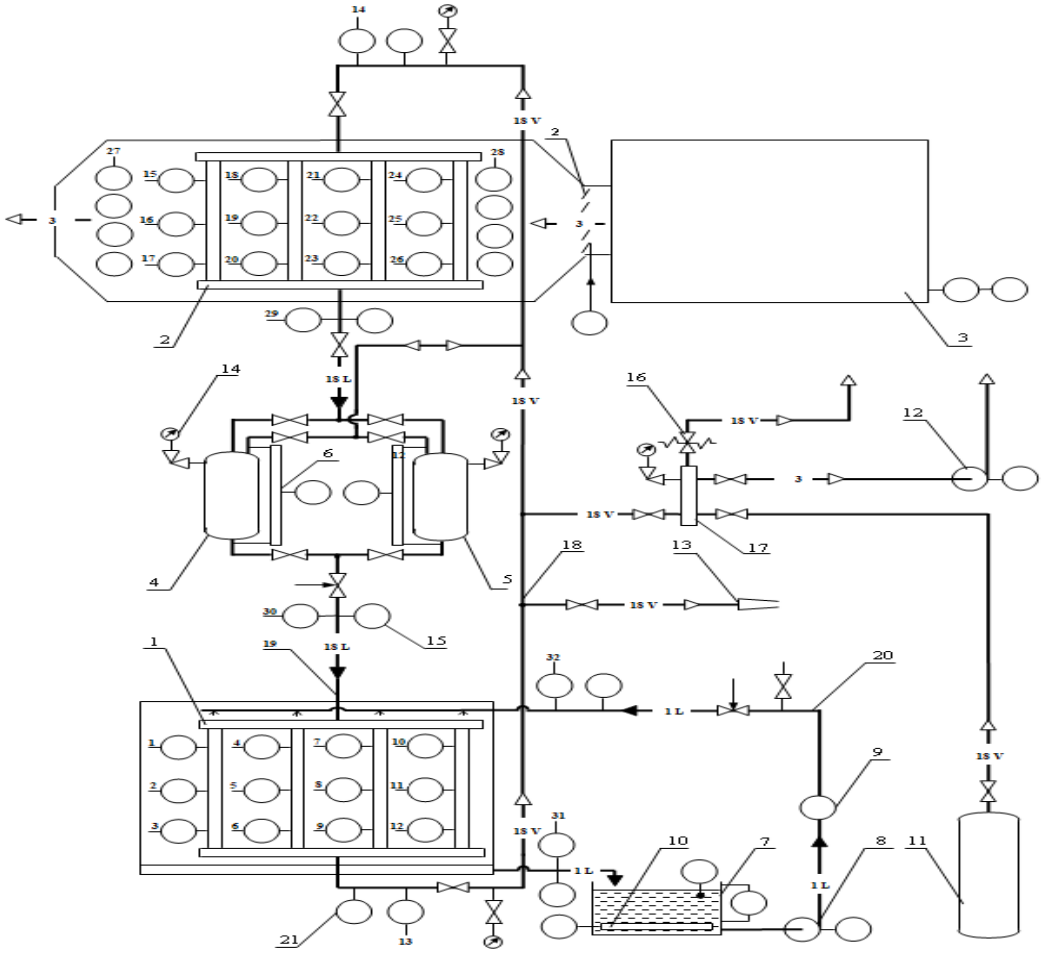

Figure 1: Experimental stand

Description of the Cold Accumulator

The cold accumulator is made in the form of a heat exchanger, with a set of 16 heat tubes of length 70 mm and 25 mm in diameter that are placed in a tank filled with water, where the upper parts of the heat pipes are placed in the evaporator, and their lower parts are installed in a water tank. An additional heat exchange surface of vertical zero sections of the same material are fixed to each of the heat pipes to increase their heat exchange area, connected to the refrigerant circulation circuit. They are placed in vertical hollow sections fixed to the outer surface of the heat tubes between the collectors at a height of H not exceeding 2/3 of the length of the heat tubes, in increments as shown in Equation 1 (Ikem *et al*., 2017).

$$X_1 = D_t + 2T + (2\delta_{th}).k; \quad (1)$$

With the axes of the collectors installed relative to the axes of the tubes at a distance as shown in Equation 2.

$$X_2 = D_t/2 + D_{coll} + T + \delta_{th} \quad (2)$$

where D_t is the heat tube outer diameter, mm; D_{coll} is the inner diameter of the collector, mm; δ_{th} is the maximum permissible ice layer thickness on the tube/collector, mm; k is safety factor taken as 1.2; T is the thickness of the hollow heat- exchange section, mm. The cold accumulator is now installed in the experimental stand in a closed refrigerant circuit loop, as shown in Figure 2.

Experimental Procedure

The following experimental procedure was provided for on the experimental stand in figure 1, given that the stand was operated in a thermosiphon mode. The evaporator 1 was flooded with hot water from tank 7 which is heated by a 6-kW electric heater 10 installed in the tank. This causes the refrigerant in the evaporator 1 to boil and its vapour goes through the refrigerants steam pipe 18, cooling as it entered the condenser 2. Here, the refrigerant vapour in finally condensed to liquid through the effect of the cold air flowing from the cooling fan 3. The refrigerant condensate from 2 is emptied into one of the liquids line receivers 4 with level indicator, while cooling water enters through valve 6 and leaving directly through valve 7, further reducing the temperature of the liquid refrigerant. At the same instance, liquid refrigerant from the tank 11 enters condenser 2, flows through line receiver 5. This will make it possible to simultaneously determine the flowrate of refrigerant through the condenser and the evaporator. The cycle continues so long as the refrigerants does not deplete.

Figure 2 shows a refrigeration unit with a cold accumulator made from heat pipes having a compressor 1, an oil separator 2, a condenser 3, a line receiver 4, a throttle valve 5, and an evaporator 6 in a closed refrigerant circulation loop.

The cold accumulator is made in the form of a heat exchanger, which is a set of heat pipes 7, placed in a tank 8, filled with water 9, which performs the function of a coolant. The upper parts 10 of the heat pipes 7 are placed in the evaporator 6, and the lower parts 11 of the heat pipes 7 are installed in the tank 8.

Pump 12 is connected to tank 8 and cold consumer 13 by a closed water circulation circuit. Inside the accumulator tank 8, a heat exchange surface is additionally fixed to each of the heat pipes 7, which is made in the form of vertical identical cylindrical hollow sections 14, connected to the collectors - supply 15 and outlet 16, connected to the refrigerant circulation circuit, respectively, by steam pipeline 17 and liquid pipeline 18. In the tank, 8 panels 14 and collectors 15 and 16 are installed on the frame 19 in the form of a single block.

In the refrigerant circulation circuit of the refrigeration unit, solenoid valves (SV) are installed.

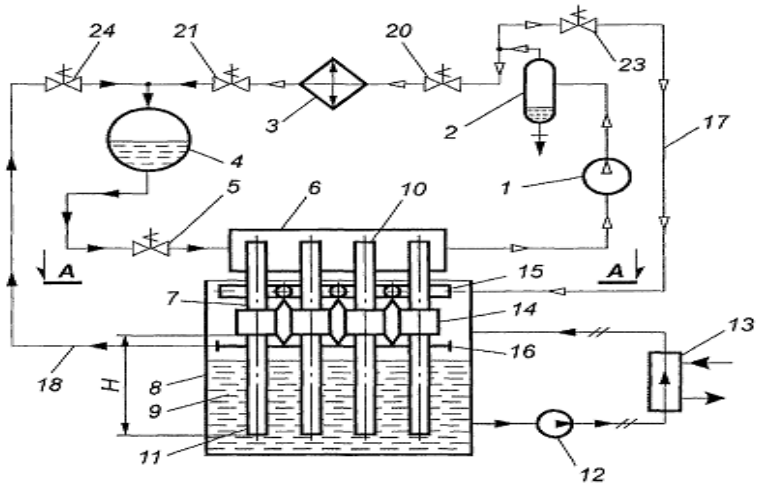

Figure 2: Schematic diagram of a refrigeration unit with cold accumulator

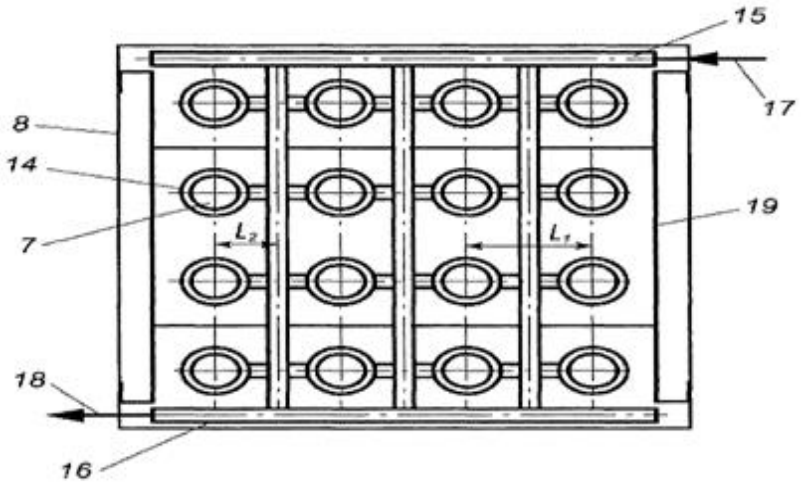

Figure 3: Schematic (section A – A) of heat pipe arrangement in cold accumulator

When the valves were properly installed and verified to be free from clogging or debris, we ensured that the power supply voltage and frequency matched the solenoid's rating, and they were connected to a calibrated test setup (water and refrigerant test stand). A 230 V AC controlled electrical input was applied to measure the coil resistance and inrush/holding current with a Multimeter. The results were compared with the manufacturer's data to ensure proper energization. Pressure/Flow Calibration: An incremental upstream pressure was applied to the valves to record the cracking pressure (the point where the valve starts to open). The full-open pressure was checked and compared with design values. Measurements of flow rate versus input signal (for proportional solenoid valves) were taken, and necessary adjustments were made for accurate measurements. Final Verification: The valves were cycled multiple times under operating conditions to ensure repeatability of actuation, and we documented and measured parameters against calibration standards.

They were installed in the refrigerant circulation circuit respectively: before the condenser - SV20; after the condenser- SV21; on pipeline 17- SV23; on pipeline 18- SV24.

A refrigeration unit with a cold accumulator of heat pipes works as follows:
Compressor 1 sucks refrigerant vapour from the evaporator and, when the SV20 is open, is pumped into the condenser 3, where the vapour condenses and, with the SV21 open, the liquid refrigerant is drained into the line receiver 4. Through the throttle valve 5, the liquid refrigerant enters the evaporator 6, where it boils, cooling the tops 10 of heat pipes 7. The cycle in the refrigerant circuit is closed.

In the evaporator 6, the heat of condensation of the antifreeze working substance with which the heat pipes are filled is transferred to the refrigerant, which flows into the lower part 11 of the heat pipes 7 placed in the tank 8, and evaporates in the lower part. On the outer surfaces of part 11, ice shells grow, which are cold accumulators. The water in the tank is cooled to a temperature of 0°C, and the cooled water from the tank 8 is taken by the pump 12 and fed to the cold consumer 13, where the process consumer is cooled, and then returned to the tank 8. The cycle in the water circulation circuit as a coolant is closed.

When an ice layer of the maximum permissible thickness δ_{th} is formed on the heat exchange surface of the lower part of the heat pipes, SV23 opens, SV20 and SV21 close, and the refrigerant vapour after the oil separator 2 is directed through the pipeline 17 and collectors 15 into the cavities of the panels 14. At the same time, when the heat of condensation of refrigerant vapour is supplied to the hollow sections 14, the circulation process of the antifreeze working fluid of the heat pipes 7 is reversed ("overturning" the operating mode of the heat pipes) by changing the direction of the flow of the antifreeze working fluid inside the heat pipe 7, after which the lower part of the pipe 11 performs the functions of an antifreeze working fluid condenser. At the same time, the heat of condensation of the refrigerant and the heat of condensation of the antifreeze working fluid ensure the thawing of the ice from the outer surface of the lower part and the heat exchange pipe 7, by completing the ice freezing process.

The thawed hollow rods of ice from the outer surface of the lower part 11 of the heat pipes 7 slide into the water filling the tank 8 without blocking the annular space, which provides free access of water to the outer surface of the lower part 11 of the heat pipes 7 during subsequent freezing.

After the hollow ice rods slide into the water of tank 8, SV24 opens, the condensed refrigerant from the

hollow sections 14 through the collector 16 and the pipeline 18 merges into the line receiver 4. SV 20 and SV 21 open, SV23 and SV24 close, the refrigerating machine begins to work in the cooling mode of the upper ends 10 of the heat pipes 7. At the same time, the normal circulation of the antifreeze working fluid inside the heat pipes 7 is restored, when the upper ends of the heat pipes 10 begin to perform the function of a condenser, and the lower ends 11 - an evaporator. The process of freezing the ice starts. Figure 3 is a section along A - A of the cold accumulator made from heat pipes. A section of the unit with cold accumulator along A - A is shown in Figure 3.

Mass of ice accumulated over one cycle

Many factors affect the performance of a cold accumulator. Consider each factor individually. The amount of ice frozen during a complete working cycle (periodic mass) m_p in kg, on the heat exchange surface is determined by Equation 3:

$$m_p = \mathrm{n}_t \times \left[\pi \times \left(\frac{D_0^2 - D_t^2}{4}\right) \times h_t + \frac{\pi . \mathrm{D}_0^2}{4}\right] \times \rho_l \qquad (3)$$

Where: n_t number of accumulator tubes; D_0 is the outer diameter of the frozen ice layer, m; D_t is pipe diameter, m; h_t is height of tube in water, m.

The following options were considered acceptable for the accumulator as determined from the simulation by this author:

n_t = 16 pcs; D_t = 0.025 m; h_t = 0.6 m; $\mathrm{D}_0 = \mathrm{D}_t + 2.\delta_{\mathrm{th}}$, m.

Where: δ_{th} is the thickness of the ice layer deposited on the tube.

Number of freezing and defrost cycles during accumulation

The number of cycles, $\mathrm{n}_{\mathrm{cyc}}$ during accumulation or defrosting is given by Equation 4:

$$\mathrm{n}_{cyc} = \frac{\tau_{ak.}}{(\tau_{fr} + \tau_{def})} \qquad (4)$$

Where: $\tau_{ak.}$ is accumulation time (at night), $\tau_{ak.}$was adopted from simulation = 8 x 3600 = 28800 s; τ_{fr} is the freezing time; τ_{def} is defrost time;

The maximum mass of the ice accumulated during the 8 hours of freezing is determined by Equation 5.

$$m_{\mathrm{ax}} = \mathrm{m_p}.\mathrm{n_{cyc}} \qquad (5)$$

Where: m_{ax} is the maximum amount of ice accumulated over the 8 hours, $\mathrm{m_p}$ is the periodic mass or mass deposited in one complete cycle and $\mathrm{n_{cyc}}$ is the number of freezing cycles.

Determination of quantity of heat used by refrigeration system

The quantity of ice accumulated during the night that can be used on production needs during the day time, reduces the condensation temperature of the refrigeration system.

The quantity of heat Q used by the accumulation period is determined by Equation 6:

$$Q = 2Q_0 + N_i \qquad (6)$$

Where: Q is the capacity of the refrigeration unit, kW; N_i is the indicated power of the compressor, kW.

Technical, economic assessment and the efficiency of refrigeration system with cold accumulator

The optimal mode of its operation was selected, characterized by an average logarithmic temperature difference of θ_m, the speed ω, of the cooling medium and the mass of the frozen ice. The part of the reduced annual cost (R-Cost) that depends on θ_m, ω and the ice thickness δ_{th} is determined by the optimal mode corresponds to the option with a minimum of the variable part of the reduced annual costs which influences the efficiency of the accumulator. A change in the inlet temperature t_0 leads to an increase in irreversible thermodynamic losses. This results in an increase in the specific power N_D/Q_o of compressor.

The value of (R-Cost), ₦/year-kW is determined by Equation (7), (ASHRAE Handbook, 2016), as:

$$RCost = \frac{[K(E_{eff} + C_n + C_p) + \tau . C_E(N_D + N_P)]}{Q_o} \qquad (7)$$

Where: K is the cost of the evaporator, ₦;

$E_{eff} = 0.16$ *is* the standard coefficient of efficiency of capital expenditures; C_n = 0.13 and $C_p = 0.06$ are portions of K, annually deducted, respectively, for the depreciation of the accumulator and its repairs; C_E *is* the cost of electricity, ₦/(kWh); N_D is the power required to drive the compressor and N_P *is* the power used in driving the water pump, respectively, kW;

Q_o *is* the cooling capacity of the refrigeration system; τ is the operating time of the refrigerating system.

We determined the value of R-Cost using five groups of options A, B, C, D, E, respectively, which correspond to the values of the boiling point $t_0 = 5, 0, -5, -10, -15$ ℃ of the refrigerant and pairing

the values of θ_m, ω and δ_{th}. For each group of options, we determined and record θ_m, Q_o, and N_e, respectively.

The system's cooling capacity Q_o is determined by Equation 8, (White, 2011)

$$Q_o = V_r \lambda_{km}(i_1 - i_{exit})/v_1 \quad (8)$$

Where: i_1 is the enthalpy of the refrigerant vapour R134a at the outlet of the evaporator and the inlet to the compressor, kJ/kg;

In order to calculate the heat transfer surface area of the evaporator, the equations of the heat flux density from the evaporating refrigerant $q_a = f(\theta_a)$ and the cooled medium $q_w = f(\theta_w)$ are solved together, where θ_a *is* the temperature head between the

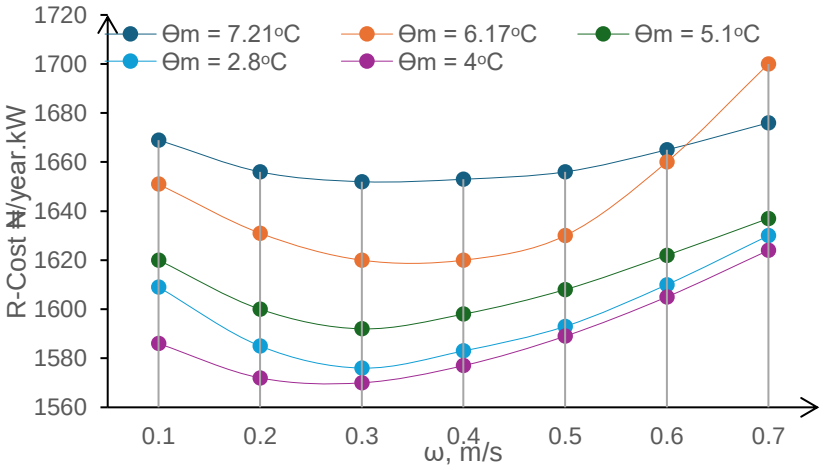

Figure 4: Variation of the optimal water speed in the accumulator

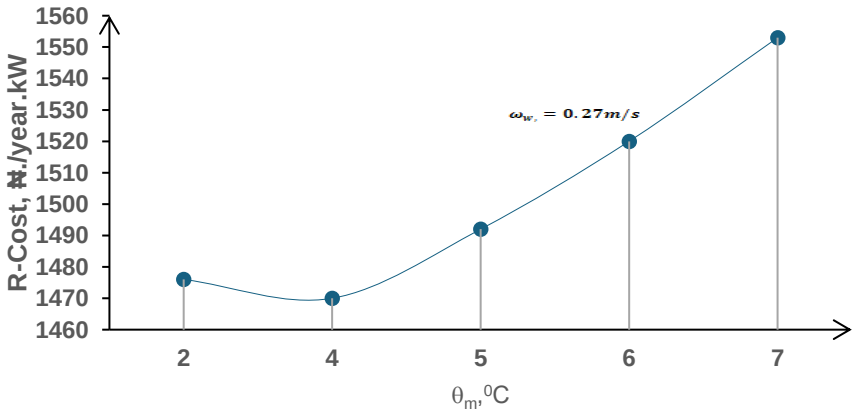

Figure 5: Determination of the optimal value of the average logarithmic temperature difference in the accumulator

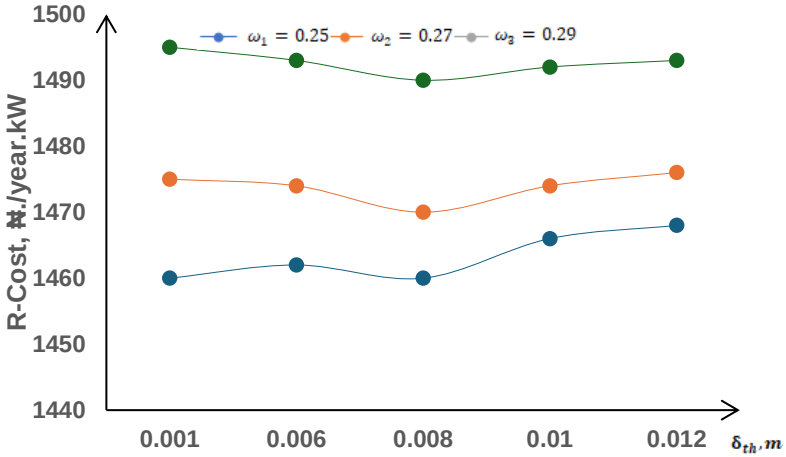

Figure 6: Variation of the optimal value of the frozen ice thickness

refrigerant and the pipe wall, θ_w *is* the temperature head between the pipe wall and the cooled medium.

The volume flow rate of water is determined by Equation 9, (Ikem *et al*, 2016):

$$V_w = Q_o/[(t_{w2} - t_{w1})C_w\rho_w] \quad (9)$$

Where: t_{w1} and t_{w2} are the water temperatures, at the inlet and outlet, ℃, respectively.

C_w is the heat capacity of water, $kJ(kgK)$; ρ_w is water density, kg/m^3.

The hydraulic resistance for water Δp, Pa, is determined by Equation 10, (Fox *et al*., 2018):

$$\Delta p = 1.34 \text{ x } Re_w^{0.82} \text{ x } n_{pr} \text{ x } n_{st} \quad (10)$$

Re_w *is* the Reynolds criterion for the flow around one row of smooth pipes (a staggered bundle); n_{pr} is the number of tube rows; n_{st} is number of strokes with a transverse flow of water around the tube bundle, formed by partitions. The pump efficiency is determined by Equation 11:

$$N_D = V_w \Delta p/\eta_P \quad (11)$$

Where: η_D is the efficiency of the pump (η_P = 0.6 is assumed).

Results and Discussion

The obtained results for the working parameters of the accumulator are presented in Table 1.

The nature of the change in the reduced costs from the parameters (Figures 4, 5, 6) showed that the optimal values of the parameters determined by the R-Cost minimum lie in the interval:

The optimum water velocity as shown in Figure 4 is ω ~ 0.25 m/s;

The temperature difference corresponding to the optimum water velocity of ω ~ 0.25 is $\theta_m = 3.5 - 4$ ℃.

Figure 6 shows the thickness of the frozen ice $\delta_{th} = 7 - 9\ mm$;

Figure 6 shows the dependences of R-Cost on δ_{th} for various values of the speed of movement of water in the accumulator, from which it follows that the dependence of the cost of freezing ice on the speed of water ω in the ice and the thickness δ_{th} of freezing ice has a weakly pronounced minimum in the range of values of δ_{th} from 7 to 9 mm, which gives grounds to recommend a working thickness of 8 mm for freezing ice. The regression for the heat transfer coefficient $\alpha, W/m^2K$ with heat flux density q, W/m^2K and boiling point of R134a is represented in Figure 7 showing that $R^2 = 0.0111q^{1.2834} = 0.9634$ and α = 0.9032 proving the adequacy of the model.

Conclusions

i). Practical data were obtained for a wide variety of temperature differential when operating a

Table 1: Parameters of the refrigerating system operation

Options	t_0℃	θ_m℃	Q_k, kW	Q_0, kW	N_D, kW
A	5	2.80	107.2	91.1	20.39
B	0	3.98	106.3	89.8	20.99
C	-5	5.11	105.4	88.5	21.58
D	-10	6.18	104.5	87.2	20.99
E	-15	7.22	103.7	86.0	22.75

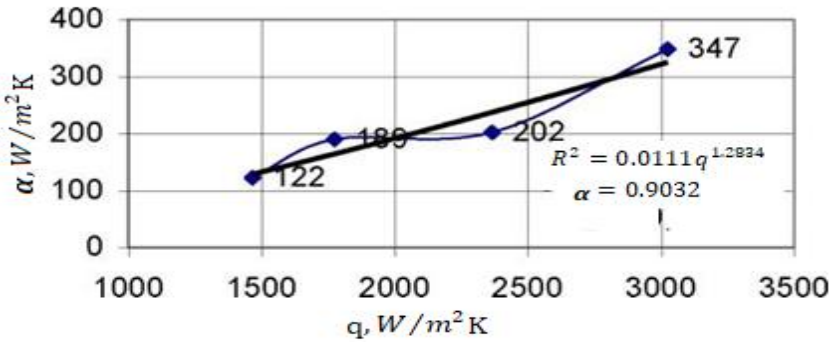

Figure 7: Variation of heat transfer coefficient $\alpha, W/m^2K$ with heat flux density q, W/m^2K and boiling point of R134a.

conventional refrigeration system incorporated with a cold accumulator.

ii). Data were obtained on the values of the heat transfer coefficients for cold accumulation, ranging from 55 to $520\,W/mK$ for heat flow from 1000 to $4000\,W/m^2$, which are approximated by the equations shown in table 4.22.

iii). It is established that the maximum performance of the accumulator takes place when ice is frozen with a thickness of about 8 mm.

iv). The amount of ice frozen during the accumulation process is sufficient to reduce the condensation temperature during the daytime peak load on the refrigeration unit by 3-4 ℃ which reduces the total energy consumption of the installation by 8-10 %.

References

ASHRAE Handbook. (2016) Arora, C.P. Refrigeration and Air Conditioning. Second edition. Tata McGraw-Hill Publishing Company Ltd. 2000.

Chen, S., Liu, X. and Fu, H. (2018). Design of Energy-saving Optimized Remote Control System of Chiller Based on Improved Particle Swarm Optimization. In Proceedings of the 2018 5th IEEE International Conference on Cloud Computing and Intelligence Systems (CCIS), 299–304.

Chia-Sheng T., Yon-Hon T., Ming-Tang T. and Chih-Liang C. (2025). The Optimal Operation of Ice-Storage Air-Conditioning Systems by Considering Thermal Comfort and Demand Response. *Energies*, 18(10), 1-16.

Dincer, I. and Rosen, M. A. (2021). Thermal Energy Storage: Systems and Applications (2nd Ed.). Wiley.

Dopazo, J. A., Fernández-Seara, J. and Sieres, J. (2012). Experimental Evaluation of a Vapour Compression Refrigeration System under Variable Loads and Variable-speed Operation. *Applied Thermal Engineering*, 33–34, 24–30.

Fox, R. W., Pritchard, P. J. and McDonald, A. T. (2020). Introduction to Fluid Mechanics (10th ed.). Wiley.

Ikem, A., I., Ibeh, M.I., Paul, O. Yusuf, Barki E., Takim, S.A. (2016). A Review of Freon 22 and Freon 134a Refrigerants in Freezing and Defrost Processes of Ice in Refrigerating Machines with Cold Accumulator. *International Journal of Engineering Trends and Technology,* 42 (6), 324 - 335.

Ikem, A., I., Ibeh, M.I., Paul, O. Yusuf, Barki E., Takim, S.A. (2017). Experimental Investigation of a Chiller with Cold Accumulator Using the Vertical Tube Evaporator Water Chiller. *International Journal of Engineering and Technology* 9 (3), 1625 –1630.

Ikem, A., I., Ibeh, M.I., Paul, O. Yusuf, Barki E., Takim, S.A. (2017). Optimization of the Energy Characteristics of a Refrigerating Machine with Cold Accumulator. *International Journal of Engineering Research*, (6)2, 47-54.

Ikem A I., Ibeh, M.I., and Ukwenya J. (2017). Estimation of the Effective Operational Mode of a Chiller with Cold Accumulator from Heat Pipes. *International Journal of Engineering and Technology*, (9)3, 1625 - 1630.

International Energy Agency (IEA) (2022). The Future of Cooling: Opportunities for energy-efficient air conditioning. Paris: IEA Publications.

Liu, X., Ma, Y. and Zhang, H. (2018). Energy Efficiency Analysis of Variable-Speed Vapour Compression Refrigeration Systems Under Part-Load Conditions. *Energy and Buildings*, 158, 1753–1761.

White, F. M. (2011). Fluid Mechanics (7th ed.). McGraw-Hill Education.

Yan, G., Liu, Y., Qian, S., Yu, J. (2019). Theoretical Study on a Vapour Compression Refrigeration System with Cold Storage for Freezer Applications.